ELSEVIER

Journal of Alloys and Compounds 323–324 (2001) 792–799

Journal of ALLOYS AND COMPOUNDS

www.elsevier.com/locate/jallcom

Correlation between spectroscopic characteristics and structure of lanthanide phosphoro-azo derivatives of β-diketones

J. Legendziewicz[a,*], G. Oczko[a], R. Wiglusz[a], V. Amirkhanov[b]

[a]*Faculty of Chemistry, University of Wrocław, F. Joliot-Curie 14, Wrocław, 50-383, Poland*
[b]*Institute of Chemistry, Kiev State of University, Vladimirskaya 64, Kiev, 2520033, Ukraine*

Abstract

Two types of lanthanide (Nd, Eu, Pr) compounds of formulae: $Ln(HX)_3Cl_3$ (**1**), $Ln(HX)_3(NO_3)_3$ (**2**) [where $HX=CCl_3CO–NH–PO(NEt_2)_2$] with the same ligand type but with different coordination numbers (as a consequence of different site symmetries) were obtained. X-ray data indicate the formation of octahedral complexes of (**1**), strongly distorted into trigonal symmetry, the strongest distortion observed for europium single crystals. On the other hand, the second type of crystals creates intermediate coordination polyhedra with low symmetry; anisotropy of intensities of $^4I_{9/2}\rightarrow{}^4G_{5/2},{}^2G_{7/2}$ transition of Nd crystal well confirms the above structure. High resolution absorption spectra of single crystals of the title compounds were recorded at different temperatures from 293 to 4.2 K. Splitting of levels was determined. Intensities of f–f transitions were calculated and changes of their oscillator strengths, in the region of hypersensitive transitions, for the series Pr, Nd, Eu crystals were related to stronger distortion of the symmetry with a decrease of the ionic radius. Oscillator strength values and Judd–Ofelt parameters were calculated and compared to the respective data reported earlier. Analysis of the electronic components in low temperature spectra point on the D_3 site in (**1**) and most probably C_{2v} in (**2**). Electron–phonon coupling was observed in low temperature spectra and its probabilities was analysed for two types of compounds with different symmetries. Vibronic components were related to the internal ligand modes and to the localised $Ln–L_x$ modes.

Keywords: Spectroscopy; Pr(III); Nd(III); Eu(III) derivatives of β-diketones; Trigonal symmetry

1. Introduction

With more extensive applications of rare earth elements in biomedicine, it has become more important to understand the behaviour of lanthanide ions in biological systems [1]. Although most of the problems are still keeping their secrets, great efforts have been made to elucidate the interactions of lanthanide ions with various biological molecules using spectroscopic methods. Sometimes, certain types of rare earth compounds, such as lanthanide chelates with phosphoro-azo derivatives of β-diketones (LnX_4), exhibit biological activities and show anticancer properties [2,3].

The same ligand can with a lanthanide ion create different types of complexes (chelating and monodentate), and so is an ideal candidate to be the subject of comparative spectroscopic investigations. Such studies can perfectly show spectroscopic effects of different kind of bonding.

Recently we reported structural and spectroscopic results for the latter (i.e., monodentate) type of compounds [4–6].

The purpose of this work is to enlarge the investigations into the other lanthanides and to study how the spectroscopic properties, which are related to crystal structure, vary from Pr to Eu, specially for the compounds with C.N. = 6.

2. Experimental

Two types of complexes, $Ln(HX)_3Cl_3$ (**1**) and $Ln(HX)_3(NO_3)_3$ (**2**) [where $HX=CCl_3CO–NH–PO(NEt_2)_2$, Ln = Pr, Nd, Eu], were prepared according to the procedure described in detail in Refs. [5,6] and single crystals of $1\times2\times3$ mm dimensions were grown.

Absorption spectra were recorded on a Cary–Varian 5 spectrophotometer equipped with a helium flow cryostat in the 293–4.2 K temperature range. The areas of the absorption bands were determined numerically (using the TAUS program) by integration and expressed in terms of the oscillator strengths:

*Corresponding author. Tel.: +48-71-3204-300; fax: +48-71-3282-348.

E-mail address: jl@wchuwr.chem.uni.wroc.pl (J. Legendziewicz).

0925-8388/01/$ – see front matter
PII: S0925-8388(01)01147-1

$$P = 4.33 \times 10^{-9} \int_{\sigma_1}^{\sigma^2} \epsilon(\sigma)\, d\sigma \quad (1)$$

where ϵ is the molar extinction coefficient of the band at wave number σ (in cm^{-1}). The experimental oscillator strengths values were used for calculation of Judd–Ofelt parameters τ_λ (cm) [7,8] according to the equation in the form given by Carnall [9]:

$$P = \sum_{\lambda=2,4,6} \tau_\lambda \sigma \left(f^N \Psi_J \| \mathbf{U}^{(\lambda)} \| f^N \Psi'_{J'} \right)^2 / (2J+1) \quad (2)$$

where $\left(f^N \Psi_J \| \mathbf{U}^{(\lambda)} \| f^N \Psi'_{J'} \right)$ are the reduced matrix elements of the unit tensor operator $\mathbf{U}^{(\lambda)}$ calculated by Carnall et al. [9] in the intermediate coupling scheme, $f^N \Psi_J$, $f^N \Psi'_{J'}$ are the initial and final states of the electronic transition, and J is the total angular quantum number. This procedure was described previously in Refs. [10,11].

The emission spectra were recorded at 40 K on the Spectra-Pro, emission line with a Xenon lamp (450 W) as the excitation source.

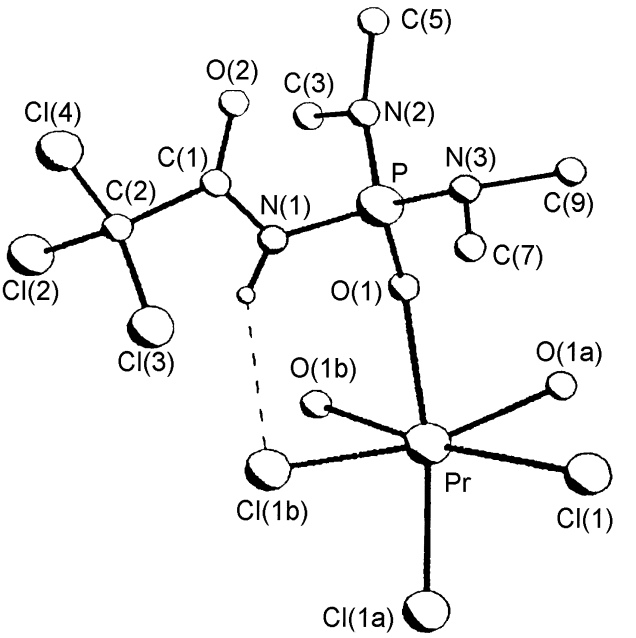

Fig. 1. Coordination polyhedron and type of ligand coordination in the structure of $Pr(HX)_3Cl_3$ (**1**) and $Eu(HX)_3(NO_3)_3$ (**2**). (Redrawn from Refs. [5,6].

3. Results and discussion

Lanthanide (Pr, Nd, Eu) title compounds obtained in the form of single crystals were checked by X-ray diffraction, confirming their isomorphism with the earlier described structures [5,6]. $Ln(HX)_3Cl_3$ crystallises in trigonal system with the $R3$ space group $Z=3$ and cell constants $a=$ 23.355(9) Å and $c=9.209(3)$ Å for Pr (III) and $a=23.485$ (69) Å and $c=9.072$ (44) Å for Eu(III). These data well confirm the decrease of the c-constant and the increase of the a-constant as the ionic radius of rare earth ions decreases. This deformation of the structure from Pr to Eu is further well manifested in spectroscopic data. Compound (**1**) creates trigonal antyprism polyhedron with symmetry close to D_3 (Fig. 1). Compound (**2**), with the $C2/c$ space group, creates a polyhedra intermediate between three capped trigonal prisms and a capped square antiprism (Fig. 1) as it was shown by the Drew method [12]. Although the same ligand type (HX) is coordinated with lanthanide ions, the second type (Cl^-, NO_3^-) modulates the crystal structure. Thus, in the chloride systems lanthanide ions have trigonal symmetry. Although from X-ray data a higher symmetric system can not be simply concluded, the spectroscopic results of $Pr(HX)_3Cl_3$ indicate the pseudocentrosymmetric system close to D_3 symmetry for praseodymium(III) compound (**1**) [4]. On the other hand, in the second $[Ln(HX)_3(NO_3)_3]$ non-centrosymmetric system, the metal ion resides at a lower symmetry.

The main purpose of this report is to show how the structural differences between systems (**1**) and (**2**) are reflected in the general features of the lanthanide absorption, excitation and emission spectra. Furthermore, emphasis in the present study is on the comparative aspect of the intensity analysis of f–f transitions, in particular their anisotropy, role of ligand polarizability and splitting of the levels at 4.2 K, electron–phonon coupling and possible transformation of the structure at low temperature, especially for the nitrate system (**2**).

Absorption spectra obtained from 293 to 4.2 K are shown in Figs. 2–4 for Pr(III), Nd(III) and Eu(III) single crystals. Tables 1 and 2 collect the results of the intensity analysis of f–f transitions performed in the values of oscillator strengths again for Nd and Eu systems (**1**) and (**2**). Similar results were reported earlier for respective praseodymium compounds [4].

The ground $^3H_4$ state of Pr^{3+} splits into $A_1+E+A_2+E+A_1+E$ in the D_3 symmetry. A_1 is supposed to be the lowest [13]. The $^3P_0$ state also belongs to the A_1 representation in the D_3 symmetry. According to the selection rule for the D_3 symmetry, transition from the lowest component of the $^3H_4$ ground term of Pr^{3+} of A_1 representation to $^3P_0$ (A_1) level is forbidden, and consequently is not detected (see Fig. 2). Transitions from higher components of the ground state are observed at room temperature (similar to the results of Richardson [14] and Schwartz [15]). In the region $^3H_4 \rightarrow {}^3P_0$ we recorded a band with energy 20 365 cm^{-1} in the spectra at 293 K [4]. It is probably the transition from higher level E ($^3H_4$) to A_1 ($^3P_0$).

The f–f transition of the lanthanides are ''parity forbidden''. In crystals they become allowed by vibronic interaction or by admixture of electronic wave functions due to odd-parity terms in the crystal field. The hypersensitive

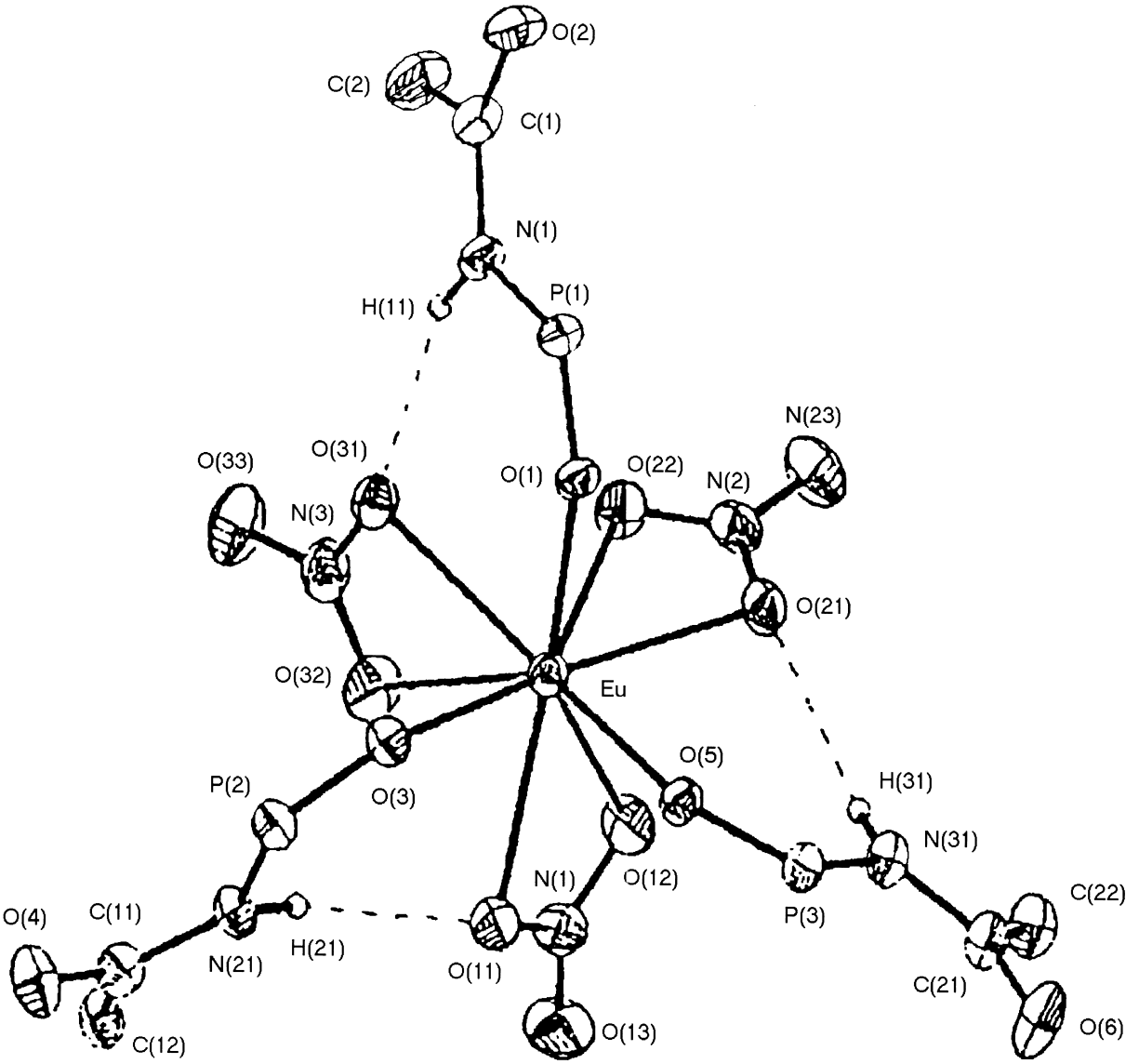

Fig. 1. (*continued*)

transitions are markedly affected by environment and their intensity can be explained in terms of both (1) the Jørgensen–Judd inhomogeneous dielectric mechanism [16] and (**2**) the Mason–Peacock–Stewart dynamic coupling mechanism [17]. On the other hand, Richardson et al. [18] calculated the intensity parameters for trigonal systems and found, except for the dynamic coupling polarizability (isotropic) term α, the dynamic coupling β, term (DC, β_L), where β_L denotes the polarizability anisotropy of ligand L. They also found a relatively strong C–T contribution in the Ω_2 intensity parameter.

In our system with a D_3 symmetry, one should consider the contributions of both terms because the chloride ions are cylindrically symmetric in a locally coordinated system and for phosphoroazo-molecules the polarizability anisotropy can be considered. This dynamic mechanism in f–f transition intensities is well manifested in changes of oscillator strength values versus temperature (see Fig. 2 and Ref. [4]). Unexpectedly, almost no changes in intensities at 293 and 4.2 K were detected for $^1D_2$ transitions in both compounds (**1**) and (**2**), usually treated as a hypersensitive ones similar to the $^3P_2$ term [4]. Moreover, at 4.2 K, the $^3H_4 \rightarrow {}^3P_0$ components become undetectable and $^3H_4 \rightarrow {}^3P_1$ is manifested as a strong sharp line in (**1**). In the praseodymium complex (**2**) all f–f bands are dramatically higher, especially for $^3F_3$, $^3F_4$, $^3P_0$ and $^3P_2$ [4], indicating second possible mechanism for non-centrosymmetric crystals, with a low site symmetry of the Pr^{3+} ion, but also the role of polarizability mechanism, because both $^3H_4 \rightarrow {}^3P_0$ and $^3P_2$ transitions vanish or very small matrix elements of $U^{(2)}$ and their hypersensitivity can be explained in the usual form of the Jørgensen–Judd theory. Calculations of Richardson [18] and Malta [19] confirm perfectly the role of the polarizability mechanism and anisotropy of polar-

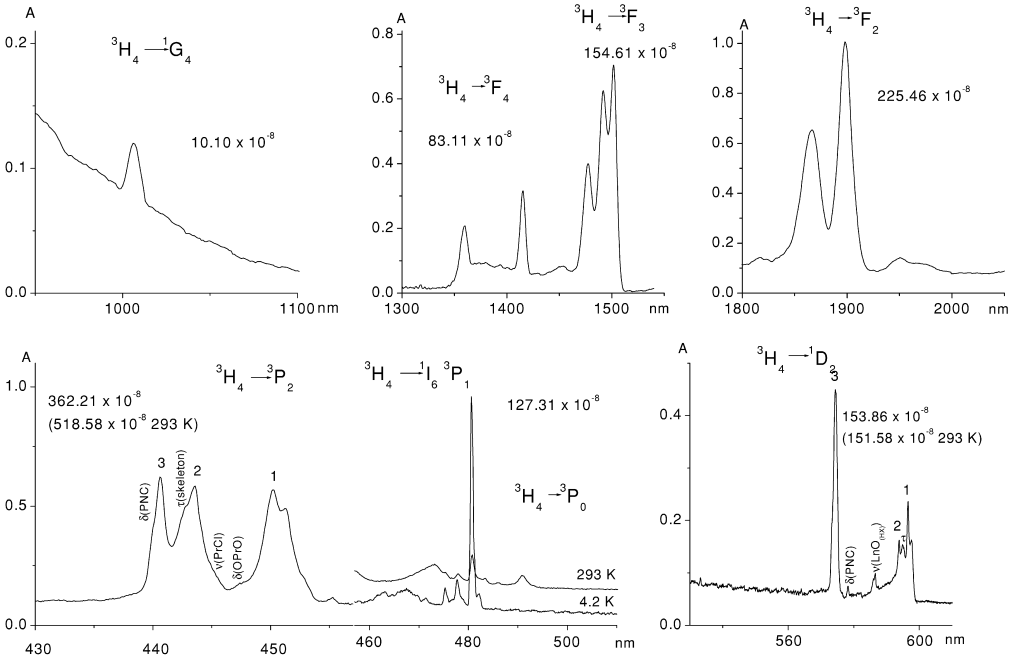

Fig. 2. The absorption spectra for a $Pr(HX)_3Cl_3$ crystal at 293 and 4.2 K with the oscillator strength values, P ($\times 10^{-8}$), of f–f transitions.

izability in explanation of $^3H_4 \rightarrow {}^3P_2$ praseodymium hypersensitivity by 2^4 and 2^6-polar contributions, which can not be neglected. It was impossible to obtain single crystals big enough and to analyse σ and Π polarised spectra for the Pr (**1**) compound and precise calculation of f–f intensities and their anisotropy.

The neodymium (**1**) and (**2**) absorption spectra at room temperature and at 4.2 K as well as $^4I_{9/2} \rightarrow {}^2P_{1/2}$ and $^4G_{5/2}$, $^2G_{7/2}$ transitions versus temperature are shown in Fig. 3. Analysis of these latter transitions make the construction of the energy level diagram of the ground state multiplet for compound (**1**) possible. Splitting of the electronic states of Nd in a crystal of (**1**) correlates well with that calculated and reported by Chowdchury for a $Nd(HAPI)_6$ cluster with D_3 symmetry at 20 K [20] and Richardson data [21]. In contrast to praseodymium (**1**) data, in neodymium (**1**) the main hypersensitive transition intensity $^4I_{9/2} \rightarrow {}^4G_{5/2}$ is relatively large. Although the intensities of two bands in IR regions: $^4I_{9/2} \rightarrow {}^4F_{5/2}$, $^2H_{9/2}$; $^4F_{7/2}$, $^4S_{3/2}$ look like those of high symmetry (e.g., O_h) systems, it means their intensities are relatively low but the decrease of temperature to 4.2 K leads to a drastic decrease of intensity for the $^4I_{9/2} \rightarrow {}^4G_{5/2}$, $^2G_{7/2}$ band only. Although from X-ray data D_3 symmetry can not be simply concluded, however such a rise from C_3 to D_3 symmetry is motivated by the spectroscopic results of the praseodymium(III) compound (**1**). Comparison of the two Nd(III) (**1**) and (**2**) systems indicates a reverse relation of intensities to those of the praseodymium (**1**) and (**2**) compounds spectra. It can be interpreted as a strong distortion of the O_h and trigonal symmetry, as a result the two and three components in the $^4I_{9/2} \rightarrow {}^4G_{5/2}$, $^2G_{7/2}$ band can be found and two of them are additionally split, pointing towards further deformation of the $NdCl_3O_3$ cluster. In other transitions, well separated lines of electric-dipole origin can be observed at 4.2 K (see Fig. 3a and b). For the neodymium system (**2**) a transformation of the structure at 160 K occurs and the low temperature spectrum reflects the new form of the neodymium nitrate complex. Table 1 collects the values of the oscillator strengths for both the neodymium system and the Judd–Ofelt parameters evaluated with very low error of estimation. In contrast to the praseodymium system, variation of the Judd–Ofelt parameters also confirms the deformation of the $NdCl_3O_3$ cluster and the strong deviation from the D_3 symmetry.

Let us consider the europium compound (**1**). As it was mentioned earlier, trigonal systems of europium (**1**) are strongly distorted. The trigonal D_3 axis coincides with the *c*-axis in (**1**). The absorption spectra of the trigonal single crystals of europium (**1**) at 293 and 4.2 K versus orientation along axes *a* (II) and *c* (III) are presented in Fig. 4. Comparison of our trigonal europium (**1**) and the spectra reported by Richardson for D_3 and C_3 trigonal systems [22] shows stronger distortion from perfect D_3 symmetry. Thus, relative transitions intensities presented in absorption and emission spectra differ somewhat from those observed by Richardson in ideal trigonal D_3 and C_3 systems [22] (see Figs. 4 and 5). In the $Na_3[Eu(ODA)_3]\cdot 2NaClO_4\cdot 6H_2O$ single crystals with D_3 symmetry $^5D_0 \rightarrow {}^7F_1$ is the strongest one and $^5D_0 \rightarrow {}^7F_2$ is almost comparable with $^5D_0 \rightarrow {}^7F_4$ transitions in the emission spectra. In our case, like above, $^5D_0 \rightarrow {}^7F_0$ is almost undetectable, but $^5D_0 \rightarrow {}^7F_1$ is lower than $^5D_0 \rightarrow {}^7F_2$ transition (see Fig. 5) [4]. Besides,

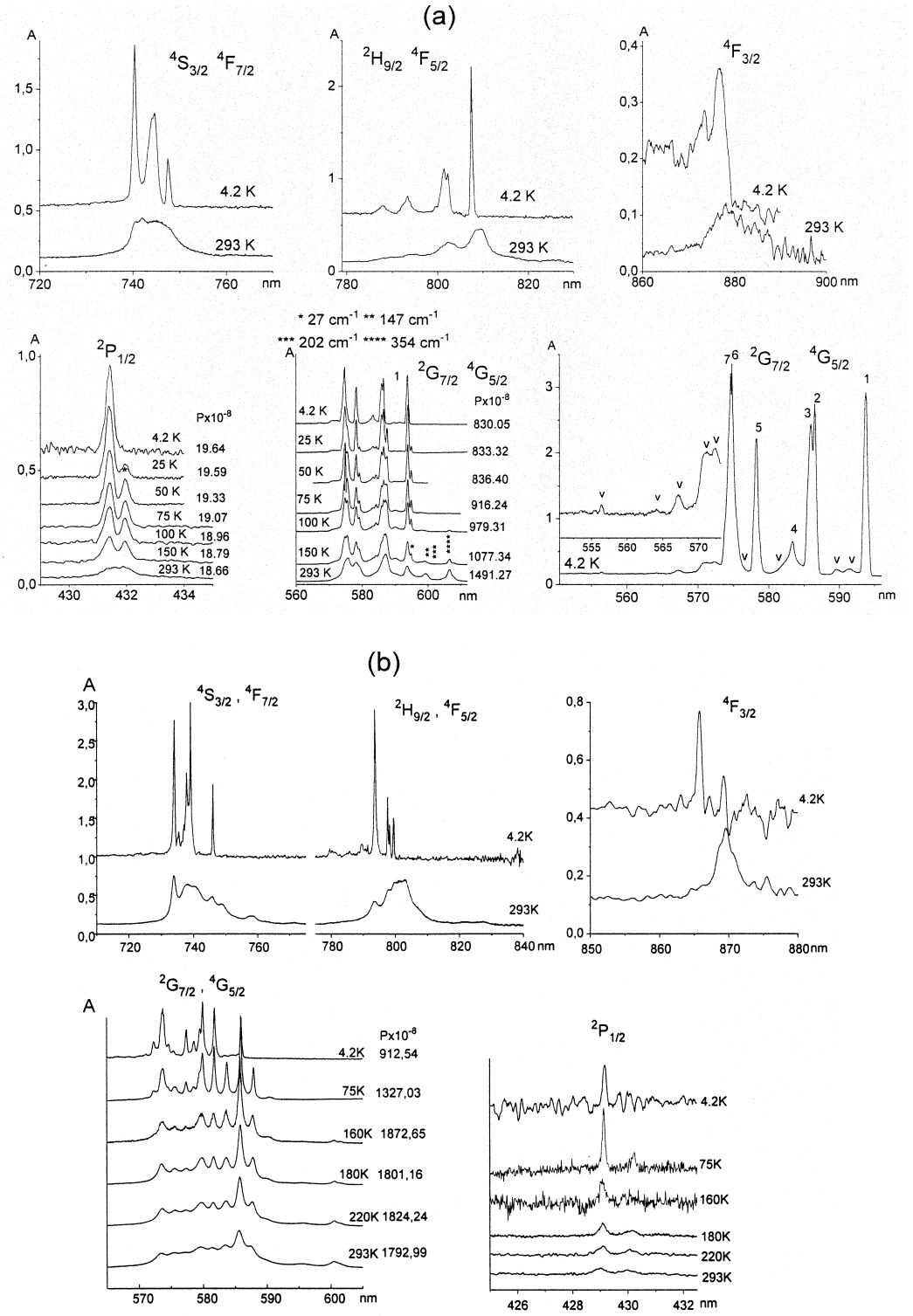

Fig. 3. The absorption spectra for $Nd(HX)_3Cl_3$ (a) and $Nd(HX)_3(NO_3)_3$ (b) crystals at different temperatures. The oscillator strength values, P ($\times 10^{-8}$) at different temperatures are given for $^4I_{9/2} \rightarrow {}^4G_{5/2}, {}^2G_{7/2}$ and $^4I_{9/2} \rightarrow {}^2P_{1/2}$ transitions and the split of the $^4I_{9/2}$ ground state is marked by asterisks.

$^5D_0 \rightarrow {}^7F_3$ is stronger than the $^5D_0 \rightarrow {}^7F_4$ transition. In fact, it can be attributed as an example of significant crystal field induced J–J mixing between $^7F_3$ and $^7F_2$ as well as $^7F_0$ and $^7F_2$ levels.

It seems important to pay attention to absorption spectra measured for two orientations of crystals along the *a* and *c* axes. Strong anisotropy of intensities is observed in an opposing relation of the $^7F_0 \rightarrow {}^5D_2$ transition compared to

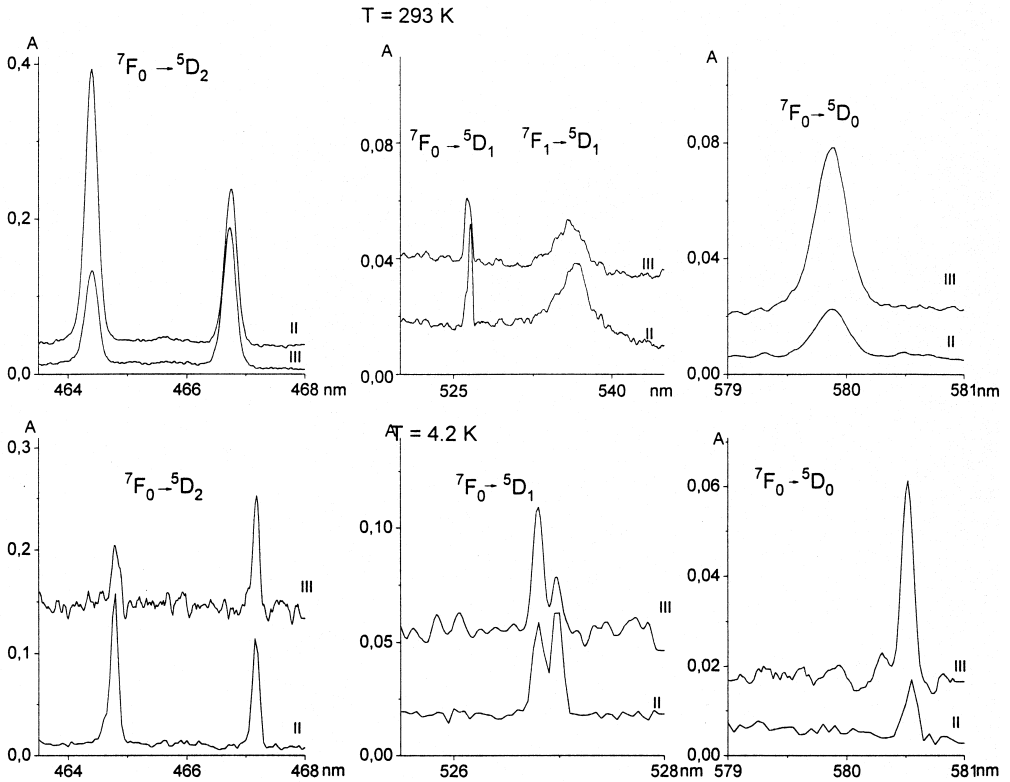

Fig. 4. The absorption spectra for the $Eu(HX)_3Cl_3$ crystal at different orientations (II,III) and temperatures.

the $^7F_0 \rightarrow {}^5D_0$ one (see Fig. 4). Moreover, at the orientation along the *c*-axis, $^7F_0 \rightarrow {}^5D_0$ dramatically increases, whereas the $^7F_0 \rightarrow {}^5D_2$ transition decreases. These changes of intensities excellently demonstrate the role of polarizability mechanism, contributing significantly in Ω_2 intensity parameters, thus it is directly related to the $^7F_0 \rightarrow {}^5D_2$ transition intensity. Since, in a mixed trigonal compound, we have two kinds of ligands: three Cl^- ions and three

Table 1
The oscillator strength values, P ($\times 10^{-8}$) of f–f transitions at different orientations (I, II) and temperatures[a]

P ($\times 10^{-8}$)	$Nd(HX)_3Cl_3$		$Nd(HX)_3(NO_3)_3$		
	293 K	4.2 K	293 K		4.2 K
			I	II	II
$^4F_{3/2}$	48.51	50.25	153.82	153.25	–
$^4F_{5/2}{}^2H_{9/2}$	177.74	140.32	494.32	659.79	587.27
$^4F_{7/2}{}^4S_{3/2}$	189.07	184.72	710.53	827.08	649.32
$^4F_{9/2}$	31.84	36.04	49.34	49.34	81.63
$^2H_{11/2}$	10.74	9.47	–	–	–
$^4G_{5/2}{}^2G_{7/2}$	1491.27	830.05	1186.87	1791.60	912.54
$^2K_{13/2}{}^4G_{7/2}{}^4G_{9/2}$	294.48	307.52	573.39	573.39	591.98
$^2K_{15/2}{}^2G_{9/2}$ $(^2D,{}^2F)_{3/2}{}^4G_{11/2}$	32.99	47.33	124.95	130.23	193.81
$^2P_{1/2}{}^2D_{5/2}$	28.98	30.43	39.06	39.06	–
$^2P_{1/2}$	18.66	19.64	15.51	15.51	9.50
$^4D_{3/2}{}^4D_{5/2}{}^2I_{11/2}{}^4D_{1/2}$	306.55	368.14	692.67	692.67	–
$^2L_{15/2}$	19.10	21.35	–	–	–
$^2I_{13/2}{}^4D_{7/2}{}^2L_{17/2}$	91.05	95.35	80.56	80.56	–
τ_2 ($\times 10^{-9}$)	7.76±0.27	–	6.16±0.46	6.16±0.46	–
τ_4 ($\times 10^{-9}$)	1.89±0.25	–	3.63±0.46	3.63±0.46	–
τ_6 ($\times 10^{-9}$)	2.06±0.35	–	8.14±0.59	8.14±0.59	–

[a] The τ_λ ($\times 10^{-9}$) (cm) parameter values were calculated from mean values of P ($\times 10^{-8}$) at 293 K for (**1**) $Nd(HX)_3Cl_3$ and (**2**) $Nd(HX)_3(NO_3)_3$ crystals. C_{Nd} = 1.1426 mol dm^{-3} for (**1**) and 1.1230 mol dm^{-3} for (**2**).

Table 2
The oscillator strength values P ($\times 10^{-8}$) of f–f transitions at different orientations (I, II) and temperatures[a]

P ($\times 10^{-8}$)	293 K			4.2 K	
$^5D_0 \rightarrow {}^7F_4$	0.56				
$^5D_0 \rightarrow {}^7F_3$	1.03				
$^5D_0 \rightarrow {}^7F_2$	25.07				
$^5D_0 \rightarrow {}^7F_1$	5.60				
Orientations	I	II	III	II	III
$^7F_1 \rightarrow {}^5D_0$		1.07			
$^7F_0 \rightarrow {}^5D_0$	0.61	0.59	1.87	0.16	0.62
$^7F_1 \rightarrow {}^5D_1$	12.81	14.21	7.78		
$^7F_0 \rightarrow {}^5D_1$	2.17	2.06	2.27	1.41	1.04
$^7F_0 \rightarrow {}^5D_2$	22.56	24.27	12.67	7.31	4.88
$^7F_1 \rightarrow {}^5D_3$	7.78	7.08			
$^7F_1 \rightarrow {}^5L_6$	7.20	6.31			
$^7F_0 \rightarrow {}^5L_6$	19.36	22.68	17.66	21.58	
$^7F_1 \rightarrow {}^5G_2$		10.53			
$^7F_0 \rightarrow {}^5G_2$	7.90	13.15		5.97	
$^7F_0 \rightarrow {}^5G_4, {}^5G_5, {}^5G_6$	8.44	13.62		8.59	
$^7F_1 \rightarrow {}^5D_4$		9.90			
$^7F_0 \rightarrow {}^5D_4$	12.79	20.37	14.44	16.13	

[a] The τ_λ ($\times 10^{-9}$) (cm) parameter values calculated from mean values P ($\times 10^{-8}$) at 293 K for $Eu(HX)_3Cl_3$ (**1**) crystal ($C_{Eu} = 1.1359$ mol dm^{-3}). τ_2 ($\times 10^{-9}$) = 4.28±0.93; τ_4 ($\times 10^{-9}$) = 2.55±1.22; τ_6 ($\times 10^{-9}$) = 0.46±0.16.

phosphoroazo β-diketone molecules, it is only in this latter molecule that anisotropy of polarizability can be responsible for the above variation in intensities.

The oscillator strengths of $^7F_0 \rightarrow {}^5D_0$ and $^7F_1 \rightarrow {}^5D_0$ calculated from absorption spectra make the calculation of oscillator strengths for $^5D_0 \rightarrow {}^7F_2$; $^7F_3$ and $^7F_4$ transitions in emission spectra possible. Thus the Judd–Ofelt parameters could be evaluated from the wide set of oscillator strengths of transitions in absorption and emission collected in Table 2. The results obtained by us are evaluated with the lowest, up to now, error of estimation. In the same table, the low temperature data for the f–f transition intensities are shown. Strong decreases in intensities for the $^7F_0 \rightarrow {}^5D_0$, $^5D_1$, $^5D_2$ transitions with temperature decrease confirms the contribution of the dynamic coupling mechanism to this systems.

The resonance effect, in vibronic coupling with the $\delta(PN_2)$ mode manifests as additional splitting (of the order of 6 cm^{-1}) of two components of the $^7F_1$ level (Fig. 5). A similar phenomenon was observed in mixed complexes of the $Eu\beta_3Ph$ type and mixed Eu carboxylates [23]. This effect was first discovered by Caro in lanthanide organic complexes [24] and Richardson [25]. Theoretical explanation of this phenomenon was given by Malta [26].

Electron–phonon coupling occurs in electronic spectra of the title compounds.

Vibronic components detected at low temperature (Figs. 2 and 3) were analysed on the basis of IR and Raman data. The modes which promote vibronic transitions are mainly associated with those groups of ligand molecules which are coordinated to the metal ions [δ(PNC), $\nu(P=O)$]. These results are in good agreement with the theory of vibronic transition probabilities.

Vibronic coupling was also found in non-centrosymmetric monoclinic systems (**2**) and will be the subject of a future paper [27].

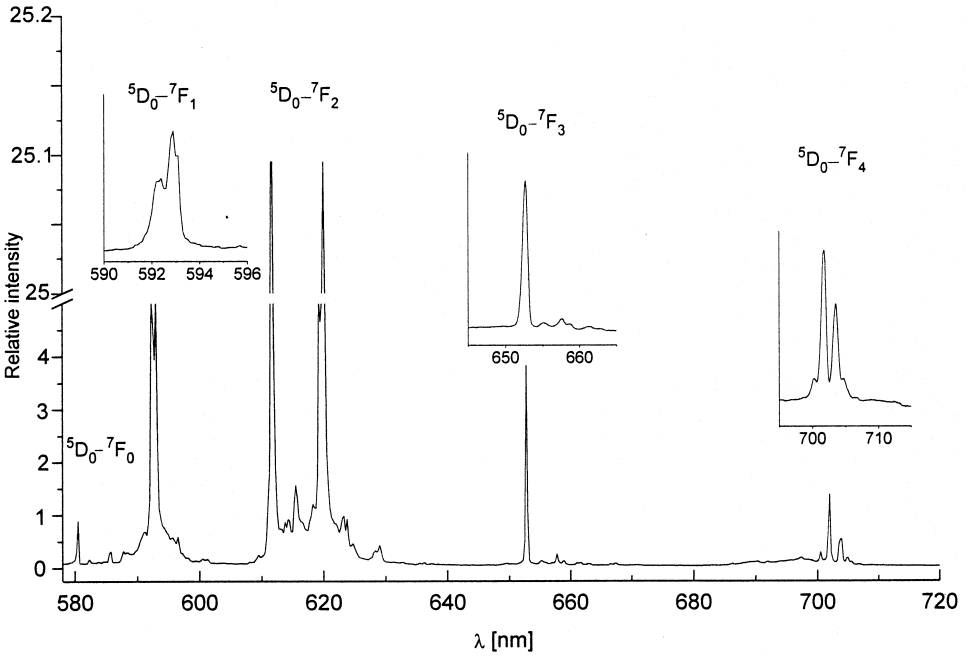

Fig. 5. The emission spectra for the $Eu(HX)_3Cl_3$ crystal at 40 K.

4. Conclusions

1. The changes in oscillator strength values versus temperature for $Pr(HX)_3Cl_3$ (**1**) and comparison of these values for both types of praseodymium compounds: $Pr(HX)_3Cl_3$ (**1**) and $Pr(HX)_3(NO_3)_3$ (**2**) indicate the contribution of the dynamic coupling mechanism as well as the role of the polarizability mechanism in f–f transition intensities.
2. The lack of the lowest component of $^3H_4(A_1)\rightarrow{}^3P_0(A_1)$ in absorption spectra of $Pr(HX)_3Cl_3$ confirms a high symmetry, closed to D_3, of the Pr^{3+} ion in this compound.
3. A relatively high oscillator strength value of the $^4I_{9/2}\rightarrow{}^4G_{5/2}$,$^2G_{7/2}$ transition for $Nd(HX)_3Cl_3$ and additionally the split of components in this band indicate a strong distortion of the O_h and trigonal symmetry and deformation of the $NdCl_3O_3$ cluster.
4. The splitting (0, 27, 147, 202, 354 cm^{-1}) of the ground state multiplet ($^4I_{9/2}$) of Nd^{3+} in compound (**1**) was determined by analysis of the $^4I_{9/2}\rightarrow{}^2P_{1/2}$; $^4G_{5/2}$,$^2G_{5/2}$ transitions versus temperature (4.2–293 K) (Fig. 3a).
5. A phase transformation of $Nd(HX)_3(NO_3)_3$ at 160 K was observed.
6. Calculation of the oscillator strengths values for a wide set of transitions in the emission and absorption spectra of a $Eu(HX)_3Cl_3$ single crystal allows the perfect calculation of the Judd–Ofelt parameters.
7. Pecularities of vibronic coupling including resonance effect was analysed.

Acknowledgements

The authors are indebted to V. Ovchinnikov for synthesis of the compounds and to Dr P. Starynowicz for X-ray confirmation of isomorphism of the investigated crystals with those of $Pr(HX)_3Cl_3$ and $Eu(HX)_3(NO_3)_3$.

References

[1] H.B. Brittain, F.S. Richardson, R.B. Martin, J. Am. Chem. Soc. 98 (1978) 8255.
[2] V. Amirkhanov, C. Jańczak, L. Macalik, J. Hanuza, J. Legendziewicz, J. Appl. Spectrosc. 62 (1995) 5.
[3] V. Amirkhanov, V. Ovchinnikov, J. Legendziewicz, A. Graczyk, J. Hanuza, L. Macalik, Acta Phys. Polon. 90 (1996) 455.
[4] J. Legendziewicz, G. Oczko, V. Amirkhanov, R. Wiglusz, V. Ovchynnikov, J. Alloys Comp. 300–301 (2000) 360.
[5] V. Amirkhanov, V. Ovchinnikov, A. Kapshuk, V. Skopenko, J. Inorg. Chim. (Rus.) 40 (1995) 1869.
[6] V. Amirkhanov, A. Kapshuk, V. Ovchinnikov, V. Skopenko, J. Inorg. Chim. (Rus.) 41 (1996) 1470.
[7] R.B. Judd, Phys. Rev. 127 (1962) 750.
[8] G.S. Ofelt, J. Chem. Phys. 37 (1962) 511.
[9] Chemistry Division, W.T. Carnall, P.R. Fields, K. Rajnak, Report (1967).
[10] J. Legendziewicz, K. Bukietyńska, G. Oczko, J. Inorg. Nucl. Chem. 43 (1981) 2393.
[11] J. Legendziewicz, Wiadomości Chemiczne 42 (1988) 605.
[12] M.G.B. Drew, Coord. Chem. Rev. 24 (1977) 179.
[13] M. Gerloch, D.J. Mackey, J. Chem. Soc., Dalton Trans. (1972) 410.
[14] F.S. Richardson, M.F. Reid, S.S. Dallara, R. D Smith, J. Chem. Phys. 83 (1985) 3813.
[15] J.P. Morley, T.R. Faulkner, F.S. Richardson, R.W. Schwartz, J. Chem. Phys. 77 (1982) 1734.
[16] C.K. Jørgensen, B.R. Judd, Mol. Phys. 8 (1964) 281.
[17] S.F. Mason, R. D Peackok, B. Steward, Mol. Phys. 30 (1975) 1829.
[18] J.J. Dallara, M.F. Reid, F.S. Richardson, J. Phys. Chem. 88 (1984) 3587.
[19] O. Malta, G.F. De Sa, Phys. Rev. Lett. 45 (1980) 890.
[20] A.F. Kirby, F.S. Richardson, J. Phys. Chem. 87 (1983) 2557.
[21] A.K. Mukhopadhyay, M. Chowdchury, Phys. Rev. B 16 (1977) 3070.
[22] A.F. Kirby, D. Foster, F.S. Richardson, Chem. Phys. Lett. 95 (1983) 507.
[23] V. Tsaryuk, V. Zolin, J. Legendziewicz, Spectrochim. Acta 54 (1998) 2247.
[24] P. Caro, O.K. Moune, E. Antic-Fidancev, M. Lemaitre-Blaise, J. Less-Common Metals 112 (1985) 153.
[25] M.T. Berry, A.F. Kirby, F.S. Richardson, Mol. Phys. 66 (1989) 723.
[26] O.L. Malta, in: Abstracts of Excited States of Transition Elements, Duszniki Zdrój, Poland, 6–12 September, 1997, p. CL14.
[27] J. Legendziewicz, J. Hanuza, E. Kucharska, G. Oczko, R. Wiglusz, in preparation.